PAPER

Check for updates

A label-free aptasensor for clenbuterol detection based on fluorescence resonance energy transfer between graphene oxide and rhodamine B

Shuyan Xiao, [ID] *[ab] Liang Sun,[ab] Mingqin Kang[c] and Zhongping Dong[ab]

A novel label-free aptasensor for the specific detection of clenbuterol was developed through the fluorescence resonance energy transfer (FRET) mechanism by using an aptamer as the target recognition element, rhodamine B (RhoB) as the fluorescence probe and graphene oxide (GO) as the fluorescence quencher. In the absence of clenbuterol, the aptamer was adsorbed on the surface of GO, preventing the interaction between RhoB and GO, and a high fluorescence signal was obtained. In the presence of clenbuterol, the aptamer specially bound to clenbuterol with a high affinity and detached from the surface of GO, while positively charged rhodamine B could be electrostatically adsorbed onto the surface of GO, thus quenching the fluorescence. By comparing the fluorescence intensity before and after the addition of clenbuterol, a simple and fast fluorescence assay for clenbuterol was established with a detection range of 100−700 nM and a detection limit of 9.6 nM. Moreover, the proposed method was successfully applied in the determination of clenbuterol in pork samples with recoveries in the range of 96.75−104.91% and a relative standard deviation of less than 5.67%. Because of its easy operation, fast response, low cost and competitive analytical performance, this method is a promising candidate for the detection of clenbuterol and can be extended to the detection of other targets by changing the corresponding aptamers.

1. Introduction

Clenbuterol is a β-adrenergic agonist that was originally developed for the treatment of asthma.[1,2] Currently, it has been illegally used as a feed additive to increase lean muscle growth and decrease fat deposition for livestock and poultry.[2] A prolonged accumulation of clenbuterol in animal tissues may cause severe threats to human health, leading to nausea, headache, dizziness, palpitations, fatigue, chills, arrhythmia and muscular tremors.[3–5] In order to ensure the safety of animal derived food, maximum residue limits (MRLs) of 0.2 ppb in fat and muscle and 0.6 ppb in liver and kidney were set for clenbuterol by the Food and Agriculture Organization of the United Nations.[6] Some countries, including the European Union and China, have banned the use of clenbuterol in animal production.[7] However, it is still illegally used in livestock as an animal growth enhancer due to economic reasons. In order to ensure food safety, the regular screening and monitoring of clenbuterol residues is necessary.

To date, a broad range of analytical techniques have been developed to detect and monitor clenbuterol, such as chromatographic approaches, electrochemical methods, immunoassays *etc.* Chromatographic approaches, including high-performance liquid chromatography (HPLC),[8,9] liquid chromatography-tandem mass spectrometry (LC-MS/MS)[10] and gas chromatography-tandem mass spectrometry (GC-MS-MS).[11] These methods are very effective and accurate, but expensive instruments and experienced personal requirements greatly limit their applications. In addition, the associated use and release of abundant organic solvents may cause environment pollution. Electrochemical methods have the advantages of a fast response, high sensitivity and easy operation, but the working electrode always needs to be modified with different materials to improve the selectivity and effectiveness of the methods. The modification process is complicated and time-consuming.[1,12–14] Immunoassays, including enzyme-linked immunosorbent assay (ELISA),[15] fluorometric immunoassay (FIA),[16,17] and electrochemical immunoassay (ECIA)[18,19] have the advantages of being simple, fast, highly sensitive and having good selectivity. However, the immunoassay methods are developed based on high-affinity and highly selective monoclonal or polyclonal antibody, and the preparation of a specific antibody is expensive, complicated and time-consuming. Moreover, the stability of antibodies is susceptible to pH, temperature and other environmental factors.[20] Therefore,

a School of Materials and Metallurgy, Inner Mongolia University of Science and Technology, Baotou, 014010, China. E-mail: xiaomdj@126.com

b Inner Mongolia Key Laboratory of Advanced Ceramic Materials and Devices, Inner Mongolia University of Science and Technology, Baotou 014010, China

c Changchun Customs Technology Center, Changchun 130062, China
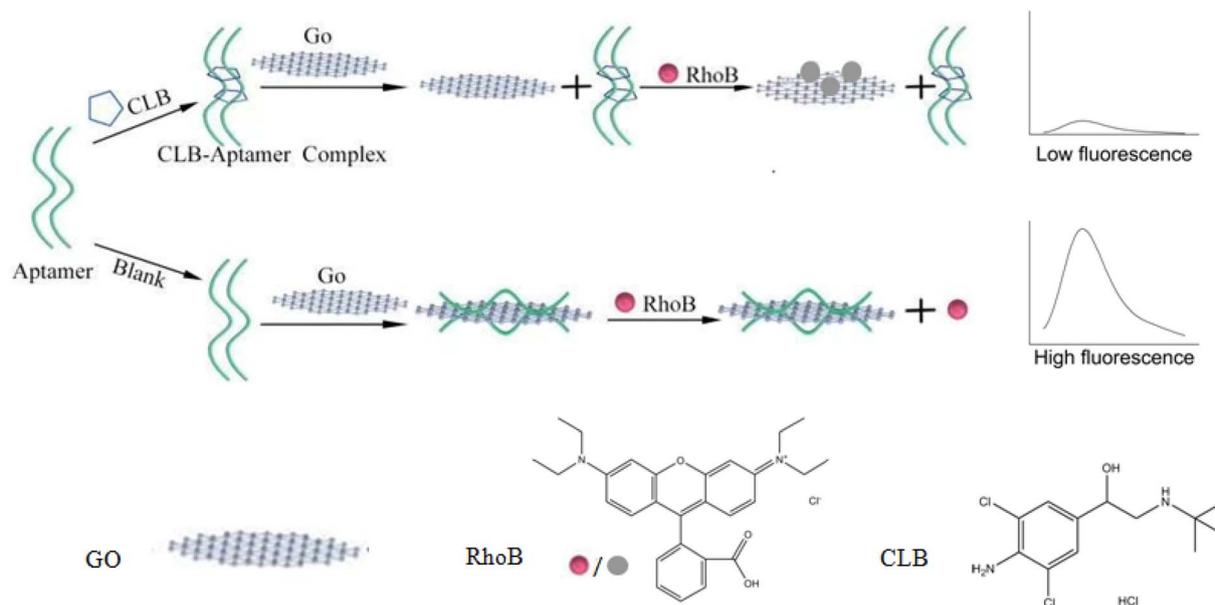
Scheme 1 Schematic illustration of a clenbuterol aptasensor based on fluorescence resonance energy transfer between graphene oxide and rhodamine B.

scientists have made great efforts to find alternatives to antibodies.

Aptamers, also known as chemical antibodies, are short chains of single-stranded DNA or RNA oligonucleotides selected from a random-sequence library by the process known as selective evolution of ligands by exponential enrichment (SELEX), which can bind to various targets with high specificity and affinity.[21,22] Aptamers, to a large extent, overcome the shortcomings of antibodies. With the advantages of a small size, low production cost, easy synthesis and modification, high stability, small batch-to-batch variability, aptamer-based biosensors have been widely developed in recent years for applications in environmental monitoring, food analysis and clinical diagnostics.[21–23]

Aptamers as recognition elements provide new insights into the detection and analysis of clenbuterol. However, since the sequences for clenbuterol binding aptamers have been screened, few studies have been carried out for clenbuterol detection, such as electrochemical,[24,25] fluorescent,[20] colorimetric[2,26] and surface-enhanced Raman spectroscopic (SERS) biosensors.[27] Many of these methods require a direct labeling process of the aptamer which results in an increased cost of synthesis and may decrease the binding selectivity and affinity of the aptamer. Hence, it is of great importance to explore label-free, simple, rapid and sensitive detection methods for clenbuterol.

In recent years, fluorescence sensors have gained much attention from researchers due to their simplicity, easy operation, quick response and high sensitivity.[28,29] Graphene oxide (GO), a two-dimensional carbon nanomaterial with a large specific surface area, has been widely used in fluorescence sensing systems as a fluorescence quencher. The fluorescence quenching mechanisms have been proposed to be associated

with a fluorescence resonance energy transfer process.[30] Moreover, GO can significantly interact with single stranded DNA through hydrophobic interactions and π–π stacking between hexagonal cells of GO and DNA bases.[31]

Herein, a sensitive clenbuterol (CLB) detection method was established by using an aptamer as the recognition element, rhodamine B (RhoB) as the fluorescence probe and GO as the fluorescence quencher. The sensing strategy of the fluorescent aptasensor is depicted in Scheme 1. Without clenbuterol, aptamers were adsorbed on the surface of GO through π–π stacking interactions between nucleotide bases and the carbon network, preventing GO from quenching RhoB, and a bright fluorescence was present. Upon the addition of clenbuterol, the formation of a clenbuterol/aptamer complex resulted in the detachment of the aptamer from the surface of GO, and the fluorescence of RhoB was significantly quenched due to fluorescence resonance energy transfer between RhoB and GO. Therefore, clenbuterol could be readily detected by monitoring the change of the fluorescence signal of RhoB from "on" to "off". The proposed approach eliminates the laborious and expensive process of DNA labeling and modification, and the detection procedure was simple and fast.

2. Materials and methods

2.1. Materials and reagents

The clenbuterol binding aptamer, 5′- AGC AGC ACA GAG GTC AGA TGT CAT CTG AAG TGA ATG AAG GTA AAC ATT ATT TCA TTA ACA CCT ATG CGT GCT ACC GTG AA-3′,[20] was synthesized by Sangon Biotech (Shanghai) Co., Ltd. Clenbuterol hydrochloride, salbutamol sulfate, terbutaline hemisulfate salt and dopamine hydrochloride were purchased from Shanghai Aladdin Biochemical Technology Co., Ltd. Tris was purchased

from Tianjin Kemiou Chemical Reagent Co., Ltd. Rhodamine B was purchased from Tianjin Beilian Fine Chemicals Development Co., Ltd. Graphene oxide was purchased from Suzhou Tanfeng Graphene Technology Co., Ltd.

2.2. Measurement procedure

A general analysis for clenbuterol was performed as follows. Twenty microliters of clenbuterol at a final concentration of 0, 100, 200, 300, 400, 500, 600, 700, 800, 900, 1000 nM was mixed with 10 μL of 3 μM clenbuterol aptamer solution, respectively, and incubated for 6 min. Afterwards, 9 μL of 20 mg mL^{-1} GO was added into the mixture and incubated for 5 min. Subsequently, 9 μL of 40 μM RhoB was added into the above solution and incubated for another 6 min. Finally, 252 μL of Tris (10 mM Tris, pH 6.5) buffer was added and the volume of each sensing system was set as 300 μL. The fluorescence spectra were recorded over the range of 550–650 nm, with an excitation wavelength of 540 nm. The fluorescence intensity at 578 nm in the absence and presence of clenbuterol was recorded as F_0 and F, respectively, and the change in fluorescence intensity was calculated as $\Delta F = F_0 - F$. The calibration curve for clenbuterol was set up by ΔF versus the concentration of clenbuterol.

2.3. Preparation of pork samples

Pork was purchased from a local supermarket and pretreated according to a procedure by Liu et al.[2] with slight modifications. One gram of pork was homogenized and then spiked with 20 μL of clenbuterol to concentrations of 3, 6, 9 nmol g^{-1}, and sonicated for 10 min. Then, the samples were blended with 0.49 mL of 0.01 M HCl, sonicated for 2 min and centrifuged at 12 000 rpm for 10 min. The supernatant was mixed with 0.49 mL of 0.01 M NaOH and centrifuged at 12 000 rpm for 10 min. Finally, the supernatant was filtered through a 0.45 μm filtration membrane and collected for further use.

3. Results and discussion

3.1. Feasibility of the fluorescent aptasensor

The proposed clenbuterol detection strategy was validated by the fluorescence spectra in Fig. 1. As can be seen, RhoB exhibited strong fluorescence in tris buffer (curve *a*) and the mixed solution containing RhoB/CLB shows negligible influence on the fluorescence properties of RhoB (curve *b*). When RhoB and GO were mixed together, the fluorescence decreased dramatically, indicating that positively charged RhoB was adsorbed onto the GO sheets through electrostatic and π–π stacking interactions,[32] and efficient FRET occurs (curve *c*). The fluorescence of RhoB/GO was still very weak in the presence of clenbuterol (curve *d*). The introduction of the aptamer in the RhoB/GO system resulted in the fluorescence being recovered to a certain extent (curve *e*), demonstrating that the aptamer can be adsorbed on the surface of GO and protects RhoB from fluorescence quenching. After the addition of clenbuterol, the fluorescence of RhoB/GO/aptamer/CLB decreased to almost the same level as that of RhoB/GO (curve *f*), indicating that almost all aptamers were removed from the surface of GO by
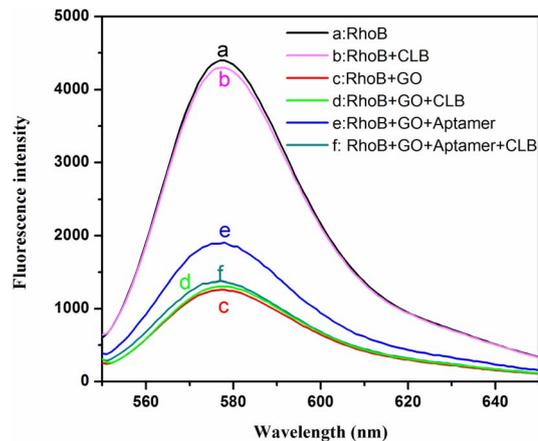

Fig. 1 Fluorescence spectra of RhoB in various systems ((a) 1.2 μM RhoB, (b) 1.2 μM RhoB + 600 nM clenbuterol, (c) 1.2 μM RhoB + 0.6 mg mL^{-1} GO: (d) 1.2 μM RhoB + 0.6 mg mL^{-1} GO + 600 nM clenbuterol, (e) 1.2 μM RhoB + 0.6 mg mL^{-1} GO + 100 nM aptamer, (f) 1.2 μM RhoB + 0.6 mg mL^{-1} GO + 100 nM aptamer + 600 nM clenbuterol).

clenbuterol. These results clearly demonstrate that the design in Scheme 1 is feasible, and the quantitative detection of clenbuterol could be easily realized by recording the changes in the fluorescence intensity of RhoB.

3.2. Optimization of sensing conditions

To acquire optimized performance for clenbuterol detection, several experimental conditions, including the pH of the solution, the concentration of RhoB and aptamer, and the incubation time between clenbuterol and the aptamer, the aptamer and GO, and GO and RhoB, were carefully investigated.

3.2.1. Optimization of the pH value. The pH value was one of the most important variables of the system because it not only influenced the surface charge of GO and RhoB, but also the interaction between RhoB and GO and between GO and the aptamer. Tris buffer with different pH values (5.5, 6.0, 6.5, 7.0, 7.5) were used to evaluate the pH influence.

As observed in Fig. 2, the variations in fluorescence intensity (ΔF) increased from 5.5 to 6.5 and then decreased. This might be due to the following reasons. On the one hand, lowering the pH reduced the negative charge density on the GO surface due to the protonation of –COO$^-$ groups, which would reduce the electrostatic repulsion with DNA aptamer.[33] Therefore, lowering the pH could promote DNA adsorption on GO and hinder the interaction between RhoB and GO, thereby reducing the fluorescence quenching efficiency. On the other hand, RhoB was positively charged in acidic solutions,[34] and lowering the pH would enhance the interactions between the RhoB and GO and improve the fluorescence quenching efficiency. The solution pH of 6.5 brought the situation into a balance and ΔF reached its maximum value, thus, this was the optimal pH value for this assay.

3.2.2. Optimization of RhoB concentration. The RhoB concentration affected both the fluorescence intensity and the sensitivity of the sensor. The larger the fluorescence difference (ΔF) between the blank and experimental groups, the higher the
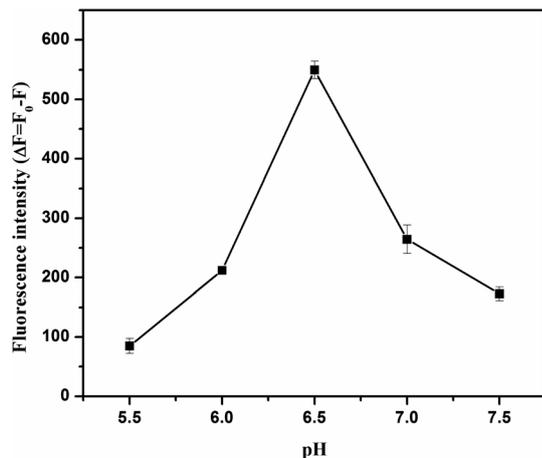
Fig. 2 Optimization of pH value. λ_{ex} = 540 nm; λ_{em} = 578 nm. The concentrations of RhoB, GO, the aptamer and clenbuterol were 1.2 μM, 0.6 mg mL^{-1}, 100 nM and 600 nM, respectively.
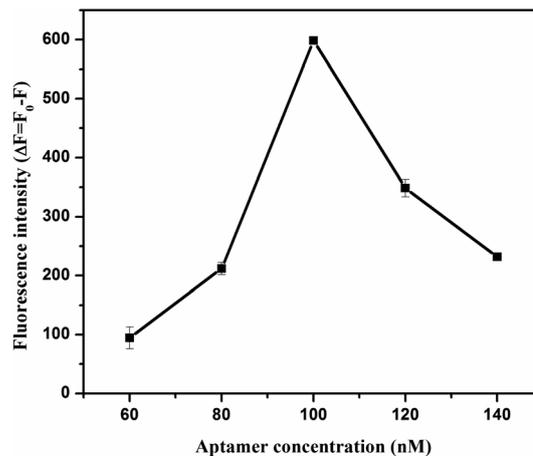
Fig. 4 Optimization of the aptamer concentration. λ_{ex} = 540 nm; λ_{em} = 578 nm. The concentrations of RhoB, GO, and clenbuterol were 1.2 μM, 0.6 mg mL^{-1} and 600 nM, respectively.

detection sensitivity will be. As shown in Fig. 3, the most significant fluorescence difference was achieved when the RhoB concentration was 1.2 μM. The reason is that if the concentration of RhoB is too low, the fluorescence intensity of the blank group and the experimental group is low, and the difference between the two groups is small. When RhoB is in excess in the sample, they would compete with the aptamer to adsorb on the surface of GO, which may lead to the partial release of the aptamer into the solution. As a result, the fluorescence difference between the blank group and the experimental group decreased. Therefore, 1.2 μM was chosen as the optimal RhoB concentration for this assay.

3.2.3. Optimization of the aptamer concentration. The concentration of the aptamer is also an important factor that affects the sensitivity and performance of the sensor. To obtain the optimal aptamer concentration, different concentrations of the aptamer in the range of 60–140 nM were tested. As shown in Fig. 4,
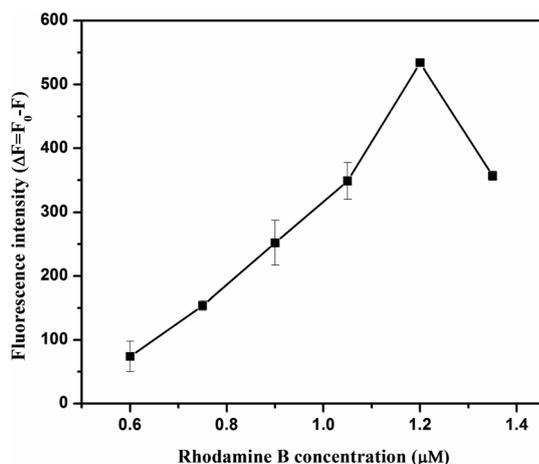
ΔF increased with increasing the aptamer concentration from 60 nM to 100 nM and then decreased, and the highest ΔF was achieved at 100 nM. A possible reason could be explained as follows. When the concentration of the aptamer is too low, the addition of clenbuterol can only remove small amounts of aptamers from the surface of GO, and the decrease in the fluorescent signal generated by clenbuterol is almost insignificant. If the concentration of aptamer is too high, the excessive aptamers in the experimental groups could also protect RhoB from GO induced fluorescence quenching and diminish the fluorescence difference between the experimental and blank groups. Therefore, 100 nM was chosen as the optimal aptamer concentration for this assay.

3.2.4. Optimization of the incubation time. The incubation time between clenbuterol and the aptamer, the aptamer and GO, and GO and RhoB were also investigated. The incubation time between GO and RhoB was set to 0, 2, 4, 6, and 8 min, respectively. As shown in Fig. 5A, the fluorescence intensity decreased rapidly with the reaction time from 0 to 6 min, and then leveled off. Consequently, the optimal incubation time between GO and RhoB was set to 6 min.

The incubation time between GO and the aptamer was set to 0, 2.5, 5, 7.5, and 10 min, respectively. The fluorescence intensity was greatly increased with the reaction time from 0 to 5 min, and thereafter, almost no changes were observed (Fig. 5B), indicating that the adsorption between the aptamer and GO was completed. Therefore, the incubation time of 5 min was selected as the optimal incubation time between GO and the aptamer.

The reaction time between the aptamer and clenbuterol was set to 0, 3, 6, 9, and 12 min, respectively. As shown in Fig. 5C, the fluorescence intensity decreased rapidly with the reaction time before 6 min and achieved equilibrium after 6 min, thus, 6 min was chosen as the optimal reaction time between clenbuterol and the aptamer.

3.3. Sensitivity and selectivity

Under the optimal experimental conditions, the sensitivity of the proposed strategy for clenbuterol detection was

Fig. 3 Optimization of RhoB concentration. λ_{ex} = 540 nm; λ_{em} = 578 nm. The concentrations of GO, the aptamer and clenbuterol were 0.6 mg mL^{-1}, 100 nM and 600 nM, respectively.
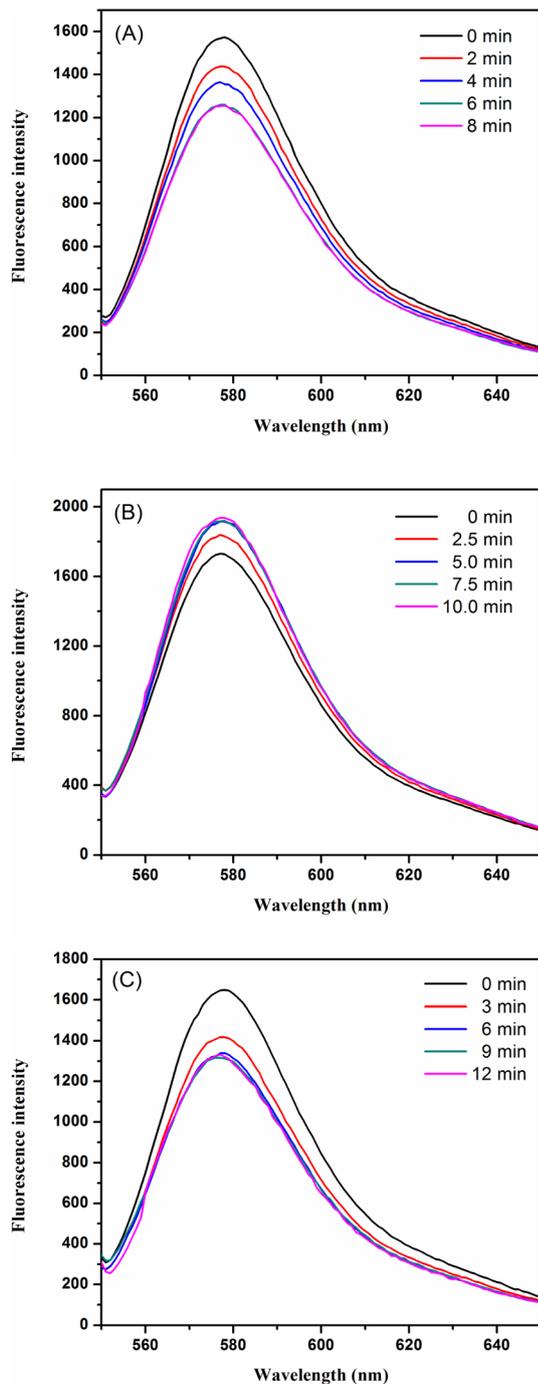
Fig. 5 Optimization of the incubation time between (A) GO and RhoB, (B) GO and the aptamer, and (C) the aptamer and clenbuterol (experimental conditions: (A) 1.2 μM RhoB + 0.6 mg mL^{-1} GO, (B) 1.2 μM RhoB + 0.6 mg mL^{-1} GO + 100 nM aptamer, (C) 1.2 μM RhoB + 0.6 mg mL^{-1} GO + 100 nM aptamer + 600 nM clenbuterol).
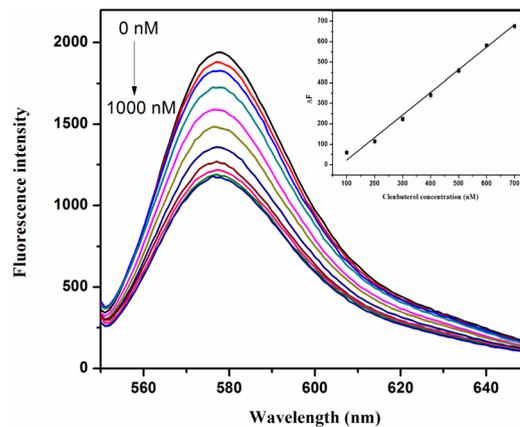

Fig. 6 Sensitivity of the aptasensor for clenbuterol detection. The inset shows the calibration curve.

The detection limit was calculated to be 9.6 nM according to the 3σ rule.[35]

In order to evaluate the selectivity of the proposed aptasensor, several interfering compounds, such as salbutamol, dopamine, and terbutaline, were detected under identical experimental conditions. It can be seen from Fig. 7 that other substances exhibited little interference toward the detection of clenbuterol, except for terbutaline, though a significant difference in ΔF between terbutaline and clenbuterol remained. Thus, the developed aptasensor exhibited good selectivity for clenbuterol detection.
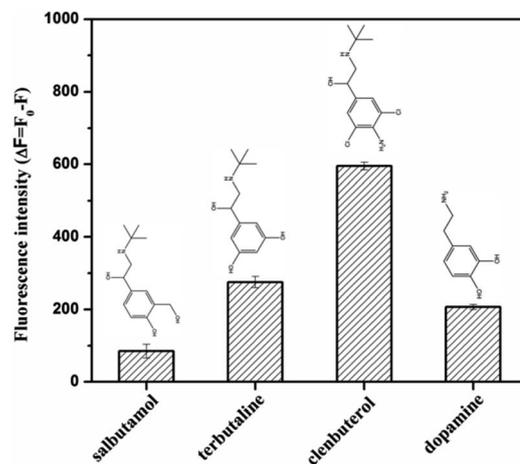

Fig. 7 Selectivity evaluation for the detection of clenbuterol (600 nM) against salbutamol, dopamine and terbutaline at the same concentration.

investigated. As shown in Fig. 6, the fluorescence intensity decreased gradually with the increasing concentration of clenbuterol, and a good linear relationship was observed between ΔF and the concentration of clenbuterol in the range from 100 to 700 nM. The linear regression equation was calculated as $y = 1.1012x - 87.4168$, with a correlation coefficient $R^2 = 0.9932$.

Table 1 Recovery of clenbuterol from spiked samples ($n = 3$)

Sample	Spiked (nM)	Detected (nM)	Recovery (%)	RSD (%)
Pork	200.00	193.50 ± 10.99	96.75 ± 5.49	5.67
	400.00	419.62 ± 8.63	104.91 ± 2.16	2.06
	600.00	587.92 ± 15.28	97.99 ± 2.55	2.60

Table 2 Comparison of different fluorescence methods for the detection of clenbuterol[a]

Material	Sample	Operation	Analytical range	LOD	Recovery	Ref.
MIP-CdTe QDs	Milk, liver	Complex	2500–22 500 nM	120 ng mL⁻¹	92–97	36
C-dots and AuNPs	Pork	Simple	8–200 nM	3 nM	97.5–105.0	28
AuNCs@BSA	Pork	Simple	4.0–300 000 nM	1.6 nM	—	37
Zr(IV)-MOFs	Water	Complex	4.0–40 ng mL⁻¹	170 nM	—	38
MIPs@UCPs	Water, pork	Complex	5.0–100.0 ng mL⁻¹	0.12 ng mL⁻¹	81.66–102.46	39
—	Pork	Simple	50–450 ng mL⁻¹	18.8 nM	90.37–104.98	40
GO	Pork	Simple	100–700 nM (31–220 ng mL⁻¹)	9.6 nM (3.0 ng mL⁻¹)	96.75–104.91	This method

[a] MIP-CdTe QDs: molecularly imprinted polymer-capped CdTe quantum dots; C-dots: carbon dots; AuNPs: gold nanoparticles; AuNCs@BSA: BSA-protected gold nanoclusters; Zr(IV)-MOFs: zirconium(IV)-based metal organic framework; MIPs@UCPs: upconversion particles coated with molecularly imprinted polymers; GO: graphene oxide.

3.4. Application to real samples

The applicability of this strategy was evaluated by pork samples spiked with different concentrations of clenbuterol. The results showed that the aptasensor would confer a recovery ratio between 96.75% and 104.91% and a relative standard deviation (RSD) between 2.06% and 5.67% (Table 1), indicating that this developed aptasensor could detect clenbuterol in pork samples with reliable accuracy.

The performance of this method was compared with other fluorescence methods (Table 2). As can be seen, the quantification range, recovery and limit of detection (LOD) of this method were comparable to other methods. Moreover, our method was simple, fast, easy to operate and cost-effective. Furthermore, the introduction of aptamer ensures the selectivity of the method. These features make it a promising tool for the rapid detection of clenbuterol.

4. Conclusion

In summary, a facile and sensitive FRET-based aptasensor for the specific detection of clenbuterol was established with RhoB as the fluorescence donor and GO as the acceptor. The presence of target clenbuterol caused desorption of the aptamer from the surface of GO. RhoB displaced the aptamer and adsorbed on the GO. As a result, the FRET between GO and RhoB was enhanced and the fluorescence emission of RhoB was turned off. Under optimal conditions, the change in the fluorescence intensity was proportional to the clenbuterol concentration over the range of 100 to 700 nM, with a LOD of 9.6 nM. The spiked recoveries for clenbuterol were 96.75% to 104.91%, with a relative standard deviation of 2.06% to 5.67% in pork samples. Promisingly, this method exhibits great potential for monitoring other targets by changing the corresponding aptamers, thanks to its easy operation, low cost and high sensitivity.

Author contributions

Shuyan Xiao: conceptualization, writing – original draft and funding acquisition. Liang Sun: investigation, methodology, data curation, and visualization. Mingqin Kang and Zhongping Dong: resources and writing – review & editing.

Conflicts of interest

There are no conflicts to declare.

Acknowledgements

References

1 L. Wang, R. Yang, J. Chen, J. Li, L. Qu and P. d. B. Harrington, *Food Chem.*, 2014, **164**, 113–118.

2 X. Liu, Q. Lu, S. Chen, F. Wang, J. Hou, Z. Xu, C. Meng, T. Hu and Y. Hou, *Molecules*, 2018, **23**, 2337.

3 J. Kang, Y. Zhang, X. Li, L. Miao and A. Wu, *ACS Appl. Mater. Interfaces*, 2016, **8**, 1–5.

4 J. Cheng, X. O. Su, S. Wang and Y. Zhao, *Sci. Rep.*, 2016, **6**, 32637.

5 N. A. A. Talib, F. Salam and Y. Sulaiman, *Sensors*, 2018, **18**, 4324.

6 B. Velasco-Bejarano, R. Velasco-Carrillo, E. Camacho-Frias, J. Bautista, R. López-Arellano and L. Rodríguez, *Drug Test. Anal.*, 2022, **14**, 1130–1139.

7 J. H. Zhao, H. C. Yuan, Y. J. Peng, Q. Hong and M. H. Liu, *J. Appl. Spectrosc.*, 2017, **84**, 76–81.

8 K. Yan, H. Zhang, W. Hui, H. Zhu, X. Li, F. Zhong, X. Tong and C. Chen, *J. Food Drug Anal.*, 2016, **24**, 277–283.

9 W. Du, S. Zhang, Q. Fu, G. Zhao and C. Chang, *Biomed. Chromatogr.*, 2013, **27**, 1775–1781.

10 K. J. Prajapati and C. Kothari, *Drug Res.*, 2020, **70**, 552–562.

11 S. Yang, X. Liu, Y. Xing, D. Zhang, S. Wang, X. Wang, Y. Xu, M. Wu, Z. He and J. Zhao, *J. Chromatogr. Sci.*, 2013, **51**, 436–445.

12 Y. Yang, H. Zhang, C. Huang, D. Yang and N. Jia, *Biosens. Bioelectron.*, 2017, **89**, 461–467.

13 Y. Ge, M. Qu, L. Xu, X. Wang, J. Xin, X. Liao, M. Li, M. Li and Y. Wen, *Microchim. Acta*, 2019, **186**, 836.

14 L. Liu, H. Pan, M. Du, W. Xie and J. Wang, *Electrochim. Acta*, 2010, **55**, 7240–7245.

15 Y. Cong, H. Dong, X. Wei, L. Zhang, J. Bai, J. Wu, J. X. Huang, Z. Gao, H. Ueda and J. Dong, *Ecotoxicol. Environ. Saf.*, 2019, **182**, 109473.

16 T. Peng, J. Wang, S. Zhao, S. Xie, K. Yao, P. Zheng, S. Wang, Y. Ke and H. Jiang, *Microchim. Acta*, 2018, **185**, 366.

17 M. A. Bacigalupo, G. Meroni, F. Secundo, C. Scalera and S. Quici, *Talanta*, 2009, **80**, 954–958.

18 Y. Lai, J. Bai, X. Shi, Y. Zeng, Y. Xian, J. Hou and L. Jin, *Talanta*, 2013, **107**, 176–182.

19 N. A. A. Talib, F. Salam, N. A. Yusof, S. A. Alang Ahmad, M. Z. Azid, R. Mirad and Y. Sulaiman, *RSC Adv.*, 2018, **8**, 15522–15532.

20 N. Duan, W. Gong, S. Wu and Z. Wang, *J. Agric. Food Chem.*, 2017, **65**, 1771–1777.

21 H. Sun and Y. Zu, *Molecules*, 2015, **20**, 11959–11980.

22 M. Ilgu and M. Nilsen-Hamilton, *Analyst*, 2016, **141**, 1551–1568.

23 Q. Kou, P. Wu, Q. Sun, C. Li, L. Zhang, H. Shi, J. Wu, Y. Wang, X. Yan and T. Le, *Anal. Bioanal. Chem.*, 2021, **413**, 901–909.

24 D. Chen, M. Yang, N. Zheng, N. Xie, D. Liu, C. Xie and D. Yao, *Biosens. Bioelectron.*, 2016, **80**, 525–531.

25 S. Huang, *Int. J. Electrochem. Sci.*, 2020, **15**, 4102–4116.

26 Y. Zhang, H. X. Ren and Y. B. Miao, *Microchim. Acta*, 2019, **186**, 515.

27 N. Duan, S. Qi, Y. Guo, W. Xu, S. Wu and Z. Wang, *LWT–Food Sci. Technol.*, 2020, **134**, 110017.

28 Y. Liu, Q. Lu, X. Hu, H. Wang, H. Li, Y. Zhang and S. Yao, *J. Fluoresc.*, 2017, **27**, 1847–1853.

29 Y. Li, R. Su, H. Li, J. Guo, N. Hildebrandt and C. Sun, *Anal. Chem.*, 2022, **94**, 193–224.

30 K. Ma, X. Li, B. Xu and W. Tian, *Anal. Chim. Acta*, 2021, **1188**, 338859.

31 X. Guo, F. Wen, Q. Qiao, N. Zheng, M. Saive, M. L. Fauconnier and J. Wang, *Sensors*, 2019, **19**, 3840.

32 R. Zhang, M. Hummelgård, G. Lv and H. Olin, *Carbon*, 2011, **49**, 1126–1132.

33 A. Lopez and J. Liu, *Adv. Intell. Syst.*, 2020, **2**, 2000123.

34 Y. J. Oh, T. C. Gamble, D. Leonhardt, C. H. Chung, S. R. Brueck, C. F. Ivory, G. P. Lopez, D. N. Petsev and S. M. Han, *Lab Chip*, 2008, **8**, 251–258.

35 J. Jia, S. Yan, X. Lai, Y. Xu, T. Liu and Y. Xiang, *Food Anal. Methods*, 2018, **11**, 1668–1676.

36 B. T. Huy, M. H. Seo, X. Zhang and Y. I. Lee, *Biosens. Bioelectron.*, 2014, **57**, 310–316.

37 X. Cao, H. Li, L. Lian, N. Xu, D. Lou and Y. Wu, *Anal. Chim. Acta*, 2015, **871**, 43–50.

38 H. Yang, B. Wang, J. Cheng, R. Wang, S. Zhang, S. Dong, S. Wei, P. Wang and J. R. Li, *Microchim. Acta*, 2019, **186**, 454.

39 Y. Tang, Z. Gao, S. Wang, X. Gao, J. Gao, Y. Ma, X. Liu and J. Li, *Biosens. Bioelectron.*, 2015, **71**, 44–50.

40 S. Xiao, L. Sun, J. Lu and Z. Dong, *New J. Chem.*, 2022, **46**, 16177–16182.